

Radiative Extinction of Diffusion Flame in Microgravity

Kuznetsov E.*, Snegirev A., Markus E.

Peter the Great St-Petersburg Polytechnic University, Saint-Petersburg, Russia

**Corresponding author's email: knOegor@gmail.com*

ABSTRACT

Forthcoming orbital experiments with the flat porous circular 25 mm diameter burner (Burning Rate Emulator) are replicated in numerical simulations of diffusion flames of ethylene and methane burning in air. The main objective is to assess the expected flame dynamics and stability, and to scrutinize the event of extinction of the unstrained diffusion flame in microgravity. For the initial period of flame development, predicted flame dynamics and the net heat flux at the burner surface are shown to be consistent with the drop tower tests performed earlier. For the longer time period to be investigated in the orbital experiments, no steady state has been predicted neither for ethylene no methane microgravity flames. Instead, the simulations have shown that flame development above the BRE burner proceeds in two consecutive modes. First, a hemispherical diffusion flame forms and expands towards a nearly spherical shape. The second mode is the evolution of the partially extinguished flame. The onset of local extinction is predicted close to the top of the spherical flame, and subsequent flame evolution is shown to depend on the fuel supply rate. In case of a small fuel supply rate, the flame self-extinguishes after several oscillations. For a higher fuel supply rate, local extinction is followed by strong re-ignition that manifests itself as an upward propagation of the triple (or hook-like) flame followed by a bright flash at the top of the flame just before complete self-extinguishment. Both symmetric and asymmetric configurations are possible.

The driving force of flame extinction is the excessive radiative heat loss rate that is not compensated by the heat release rate in the reaction zone. The ethylene flames exist for a longer time period than the methane flames, in spite of comparable radiative emission. The flames produced by a lower fuel supply rate are shown to be more stable and it could exist for a longer time.

The simulations have shown that gas radiation dominates over that of soot. When the classical WSGG model is applied to evaluate the effective absorption coefficient of the gaseous combustion products, selection of the mean radiation pathlength strongly affects the prediction of radiative emission from flame and its lifetime prior to extinction.

KEYWORDS: Flammability, extinction, microgravity, diffusion flame.

INTRODUCTION

The long history of orbital studies of diffusion flames in microgravity includes experimental and theoretical investigations of droplet combustion, flame spread, jet and candle flames etc. [1]. At the same time, dynamics and stability of diffusion flames developing in microgravity in the quiescent atmosphere above a flat fuel source have not been thoroughly addressed, in spite of its direct relevance to the flammability of solid materials.

Burning of a combustible material proceeds as a result of the close, non-linear, two-way interaction between the heat flux generated by the gaseous flame and thermal decomposition of the material. The inherent complexity of thermochemical phenomena occurring in burning of solid combustibles impedes direct measurement of critical mass flow rates at flame ignition and extinction. It is

Proceedings of the Ninth International Seminar on Fire and Explosion Hazards (ISFEH9), pp. 214-224

Edited by Snegirev A., Liu N.A., Tamanini F., Bradley D., Molkov V., and Chaumeix N.

Published by St. Petersburg Polytechnic University Press

ISBN: 978-5-7422-6496-5 DOI: 10.18720/spbpu/2/k19-73

therefore instructive to develop a methodology that decouples the flow rate of pyrolysis volatiles from the flame properties, yet enabling control over the characteristics of the volatiles and the burning surface.

This idea is implemented in the Burning Rate Emulator (BRE), a flat burner designed to emulate the burning behavior of liquids and solids by supplying a controlled gaseous fuel flow [2, 3, 4]. The burner represents a liquid or solid fuel through the four key properties: heat of combustion, heat of gasification, vaporization (surface) temperature, and laminar smoke point. Fuel supply rate is decoupled from the heat flux incident to the burner surface, thereby enabling accurate measurements of the critical value at extinction. Thus, the BRE can be used as a tool to determine the flammability conditions for certain materials in terms of the four above-listed characteristic properties.

Previous work undertaken in normal gravity [3, 5] and in short-duration (few seconds) microgravity in NASA Glenn drop tower [2, 4] supports this concept. Need to consider the long-term transient flame development and to examine ability of the flame to approach a steady state is the motivation behind the orbital BRE-Flamenco experiment included in the ACME program [6, 7, 8].

Extinction of an unconfined laminar diffusion flame is known to be driven by either high strain (blow-off) or by excessive radiative heat losses from the reaction zone (quenching). For a given composition of the fuel and oxidizer streams, the critical bounds of local strain exist, and steady burning is only possible when the local strain (and, therefore, the residence time available for the reactants entering the reaction zone) is within the above bounds (for example, see Ref. [9]).

Note that the experimental conditions corresponding to the low-strain (radiative) extinction limit cannot be replicated in normal gravity, which generates considerable buoyancy-driven velocity strain that controls both the residence time and the inner structure of the diffusion flamelet. This motivates the experimental studies undertaken in the drop tower tests and in the orbital flight.

The objective of this work is to replicate the conditions of the forthcoming experiments in numerical simulations, to attempt predicting the flame dynamics and stability, and to scrutinize the event of flame extinction. Specific objectives also include developing and validation of the Fluent-based methodology for predicting laminar diffusion combustion in normal and microgravity, comparing different fuels (methane and ethylene), and investigating the effects of the radiative losses on the extinction dynamics at different fuel supply rates. The simulation program is designed to provide guidance for ISS onboard experiments with the BRE setup.

MODEL SETUP

Numerical approach

The simulations were performed using ANSYS Fluent 18.2 software. The following solver settings were used:

Pressure-velocity coupling:	Coupled scheme
Spatial discretization:	
Gradient	Least squares cell-based
Pressure	Second order
Momentum and scalars	Second order upwind
DO	First order upwind
Transient Formulation:	Bounded second order implicit
Stiff Chemistry Solver (ISAT, integration parameters as default in Fluent)	
Transient solver (0g BRE flames):	0.2 ms time step, 10 iterations per time step
Steady solver (1g laminar diffusion jet flames)	

Reduced chemical mechanism DRM22 (22 species, 104 reactions) by A. Kazakov and M. Frenklach [10] is used for combustion of methane, and the skeletal mechanism by Z. Luo et al. [11] (based on USC-Mech II, 32 species, 206 reactions) is used for combustion of ethylene. Both mechanisms are uploaded using the Chemkin-import option. Thermochemical and transport data from GRI-Mech 3.0 are applied. The Moss-Brooks soot formation model (precursor is instantaneous C_2H_2) is utilized jointly with the Fenimore-Jones soot oxidation model (instantaneous OH). Thermal radiation transfer is modeled by the discrete ordinates (DO) method, and the gas-soot mixture effective absorption coefficient is evaluated using the Weighted Sum of Gray Gases (WSGG) model, with the user-specified mean radiation pathlength.

Geometry and meshing

The BRE setup with 25 mm diameter flat circular burner is considered. In the simulations, the burner outlet is elevated 25 mm above the bottom boundary.

The computational domain consists of two coaxial cylinders connected at a plane surface containing the burner outlet surface (see Fig. 1). The lower part of the domain surrounds the burner and has the external diameter of 120 mm. The upper part of the domain is of 10.5 cm height and 160 mm diameter.

Vertical (side) and upper boundaries are set open (“pressure-outlet” boundary in ANSYS Fluent). Bottom boundary and burner side are kept at a constant temperature 300 K (“wall” boundary). Uniform fuel inlet velocity profile is applied at the burner outlet, with the mass flow rate varied in the range from 2 to 10 $g/(m^2 \cdot s)$, corresponding to the mass loss rates of burning solid fuels. Two gas fuels, methane and ethylene, are considered. Burner surface temperature and that of the fuel outflow is set at 300 K. The initial ambient temperature is also set at 300 K.

Block-structured hexahedral mesh (2.543 million cells, 0.25 – 0.38 mm characteristic cell size in the Cartesian rectangular inset above the burner) is used in the simulations. The cell size increases at the periphery of the computational domain as shown in Fig. 3 by the grid lines in the vertical axial plane and in the horizontal cross-section. In the separate study, Ref. [8], we have shown that this spatial resolution is sufficient to replicate the structure of the normal gravity laminar jet diffusion flame of methane in the air co-flow presented in NIST experimental archive, Ref. [12]. In microgravity, the unstrained flame is thicker than that in the strained flame developing in normal gravity, and the thickness of a growing flame increases in time. It justifies the mesh resolution used in this study, although further investigation of mesh sensitivity is in progress.

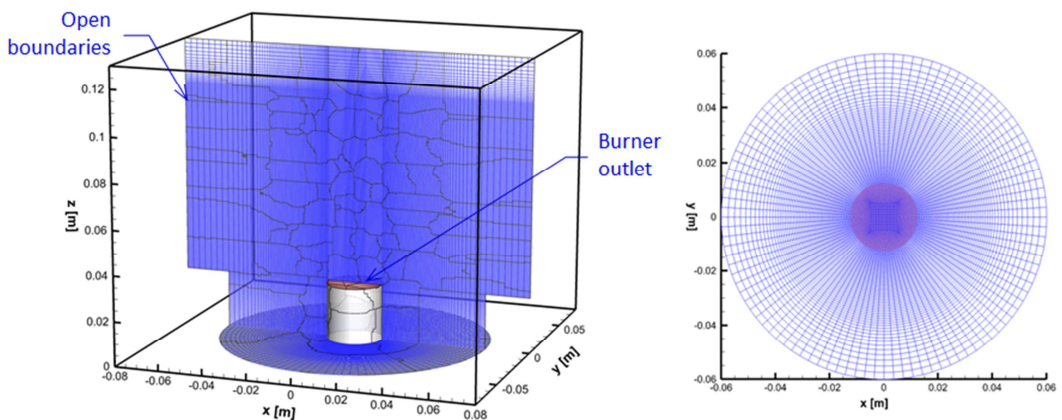


Fig. 1. Computational domain and mesh.

Method of ignition

To ignite the fuel, a sufficiently high temperature is required in the region of stoichiometric fuel to air ratio. In the experiments, either a pilot flame or an electric spark are used; in the simulations, an approximate model of pilot ignition is required. Two approaches are applied in this work to simulate ignition:

1. The fuel inlet temperature is set at 2000 K (mass flow rate $5 \text{ g}/(\text{m}^2 \cdot \text{s})$) for 0.04 sec. By the end of this period, a hot gas core is formed near the burner outlet (see the left plot in Fig. 2, a). This dataset is used as the initial condition for subsequent transient simulations with the fuel flow parameters of interest. It was noticed that, although this hot core is sufficient to initiate the flame growth in 0g, no steady flame is predicted in 1g conditions. In the latter case, the hot core is quickly dispersed by the cold air entrained by the uprising buoyant flow. It can, therefore, be concluded, that such a hot spot is more hazardous in 0g than in 1g.
2. The second approach replicates the experimental conditions of the drop-tower experiments [2]. Initially, the steady buoyant diffusion flame is simulated for the given fuel flow rate in normal gravity (see the left plot in Fig. 2, b). This dataset is then used in the transient simulations performed in zero gravity. Consistent with the drop tower experiments, Refs. [2, 4], the simulations have shown that the flame quickly (in about 1 s) transforms to its hemispherical microgravity shape.

After the short transitional period of about 1 s, both of the above approaches produce similar predictions of flame shape (see the right plots in Fig. 2).

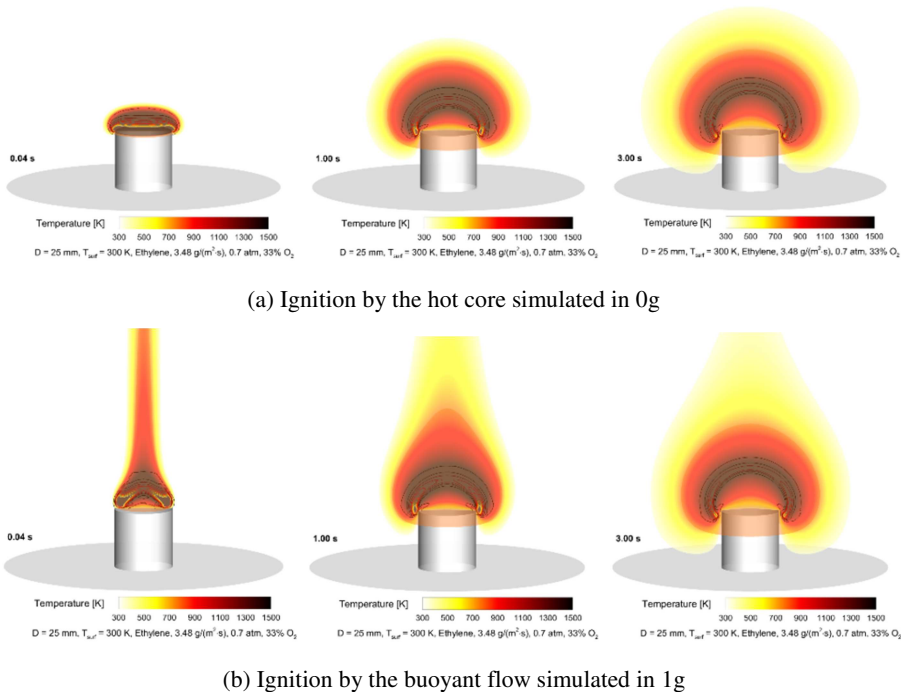


Fig. 2. Instantaneous flame structure at time instants 0.04, 1 and 3 s (left to right) shown by the temperature distribution and the iso-curves of the heat release rate (solid lines) in the axial plane. Simulation results are presented for two methods of ignition.

BRE FLAMES IN MICROGRAVITY

Drop tower tests

The tests were performed at NASA Glenn's 5-s zero gravity research facility for two burner diameters (25 mm and 50 mm) with methane and ethylene fuels as described in Refs. [2, 4]. Videos of the tests are available in the archive [14]. To validate the numerical predictions, the test with ethylene supplied at the rate of $3.48 \text{ g}/(\text{m}^2 \cdot \text{s})$ in the atmosphere with a high oxygen content (33% O_2) at an ambient pressure of 0.7 bar is replicated in the simulations.

The simulations predict formation and expansion of the hemispherical flame with the shape and the growth rate similar to that observed in the experiment (see Fig. 3). Furthermore, Fig. 4 shows a very good agreement between the measured and simulated net heat flux received by the burner surface during the zero gravity period from 0 to 5 s. This observation (as well as the normal gravity simulations for the laminar jet flame, Ref. [9]) indicates validity of the numerical approach, at least during the initial period of flame growth.

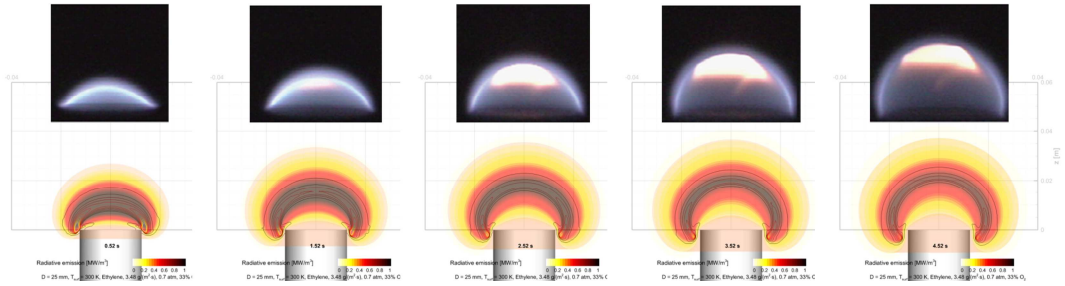


Fig. 3. Drop tower microgravity test with 100% C_2H_4 , $3.48 \text{ g}/(\text{m}^2 \cdot \text{s})$, 33% O_2 , 0.7 bar. Upper photos: experimental images at time instants 0.5, 1.5, 2.5, 3.5, and 4.5 s [2]. Lower plots – predicted temperature distributions and heat release rate iso-curves in the central plane at the same time instants.

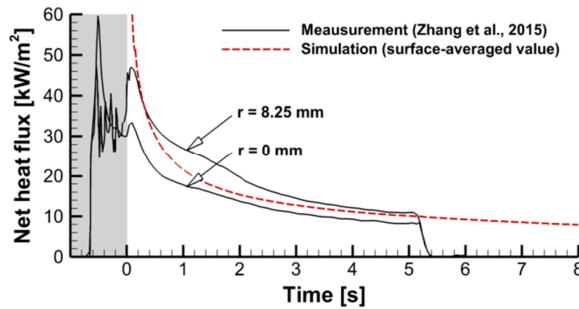


Fig. 4. Transient variation of the net heat flux at the burner surface. 100% C_2H_4 , $3.48 \text{ g}/(\text{m}^2 \cdot \text{s})$, 33% O_2 , 0.7 bar.

For a steady-state spherical flame, the stagnant film theory predicts the following flame radius

$$R_f = \left(\frac{\dot{m}_{fuel} c_{p,2}}{4\pi k_2} \right) / \ln \left(1 + \frac{c_{p,2} (T_f - T_\infty)}{(1 - f_r) \Delta h_c - c_{p,vap} (T_f - T_s)} \right) \approx \frac{\dot{m}_{fuel}}{4\pi k_2} \frac{1}{T_f - T_\infty} (1 - f_r) \Delta h_c, \quad (1)$$

where \dot{m}_{fuel} is the fuel supply rate, k_2 and $c_{p,2}$ are the thermal conductivity and constant pressure specific heat of ambient air, T_f and T_∞ are the flame and ambient temperatures, Δh_c is the heat of

combustion, and f_r is the radiative fraction. Eq. (1) indicates that the steady flame radius is proportional to the fuel flow rate. However, the simulations show that the growing flame may not approach the steady state due to the extinction, which is induced by the radiative losses. Indeed, the simulations performed for the longer time period reveal steady flame growth followed by the extinction at 16 s after ignition (see Fig. 5). The following conclusions can be made. The shape of the expanding flame is almost perfectly spherical. As the flame grows, the peak temperature in the reaction zone steadily decreases down to the very low values of about 1200 K. Local flame extinction occurs at the flame top at about 15.5 s, while the bottom edge of the flame still burns. Re-ignition results in propagation of premixed flame upwards. As the edges of the propagating flame collide, the intensive flash occurs, which is followed by complete flame extinguishment. This phenomenon is investigated in more details in the subsequent sections of the paper.

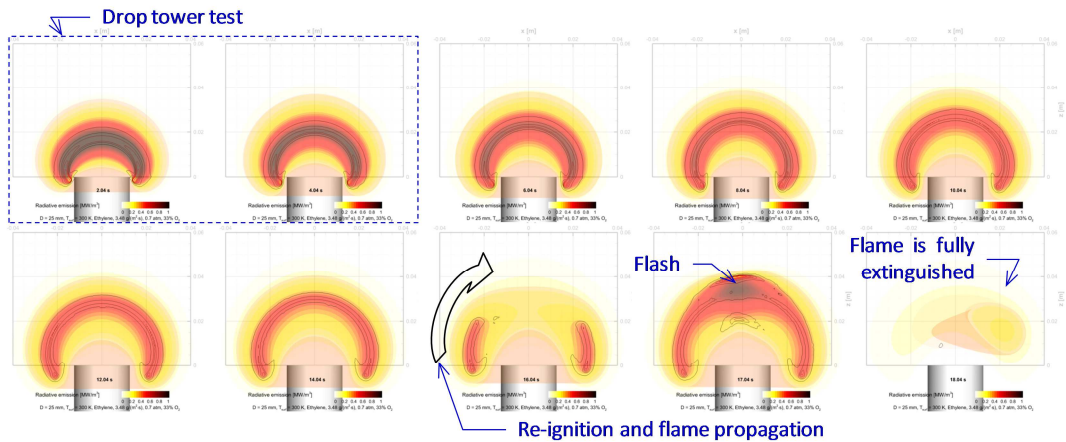


Fig. 5. Predicted temperature distributions and heat release rate iso-curves in the central plane at the time instants 2, 4, 6, 8, 10, 12, 14, 16, 17, and 18 s (100% C_2H_4 , $3.48 \text{ g}/(\text{m}^2 \cdot \text{s})$, 33% O_2 , 0.7 bar).

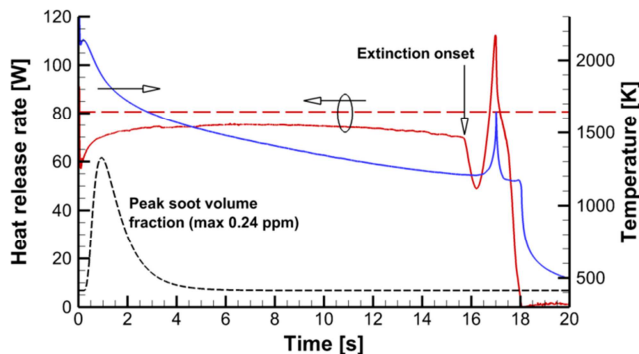


Fig. 6. Predicted transient variations of total heat release rate, peak temperature, and peak soot volume fraction (100% C_2H_4 , $3.48 \text{ g}/(\text{m}^2 \cdot \text{s})$, 33% O_2 , 0.7 bar).

Transient development and extinction of BRE flames at 0g

Here we consider the BRE flames predicted at zero gravity in the air (0.21 O_2 , 0.79 N_2 mole fractions) at the pressure of 1 bar. Pure ethylene and methane flow rates of 2 and $10 \text{ g}/(\text{m}^2 \cdot \text{s})$ are considered, and predicted flame dynamics for the ethylene flames is shown in Figs. 7 and 8.

The overall flame dynamics is qualitatively similar to that described above. After ignition, radius of the spherical flame grows almost linearly in time. The radiative losses increase, and the peak temperature steadily decreases from the initial value of 2100–2200 K to about 1200 K (Fig. 9). Note, that such a low flame temperature is consistent with the theoretical analysis for the radiative extinction limit in Ref. [9]. Eventually, local extinction is observed, which manifests itself in appearance of the hole at the top of flame ball as shown in Figs. 7 and 8.

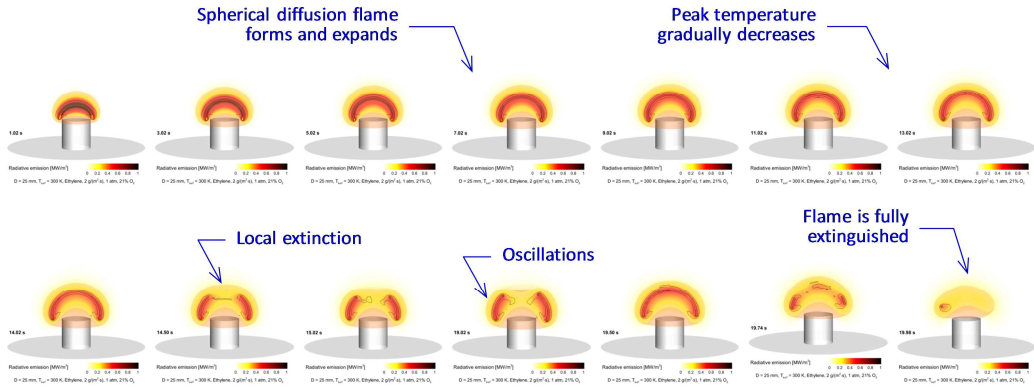


Fig. 7. Predicted temperature distributions and heat release rate iso-curves in the central plane at the time instants 1, 3, 5, 7, 9, 11, 13, 14, 14.5, 15, 19, 19.5, 19.7, and 19.9 s (100% C₂H₄, 2 g/(m²·s), 21% O₂, 1 bar).

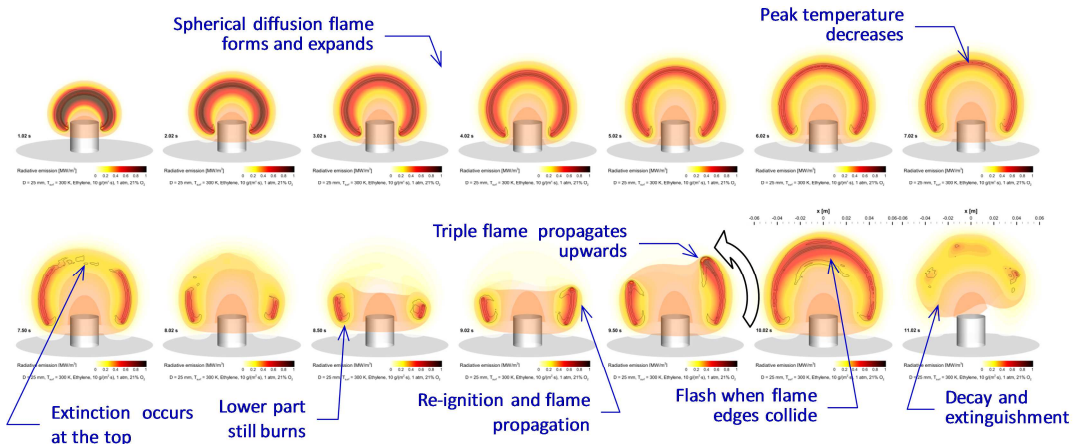


Fig. 8. Predicted temperature distributions and heat release rate iso-curves in the central plane at the time instants 1, 2, 3, 4, 5, 6, 7, 7.5, 8, 8.5, 9, 9.5, 10, and 11 s (100% C₂H₄, 10 g/(m²·s), 21% O₂, 1 bar).

Further flame evolution depends on the fuel flow rate. At sufficiently low fuel flow rates (e.g. 2 g/(m²·s)), the hole size and total heat release rate in the flame oscillate in time with the growing magnitude as shown in Fig. 9, a. After several oscillations, the flame is completely self-extinguished. Alternatively, at a high fuel flow rate of 10 g/(m²·s), just one cycle occurs before the flame is completely extinguished. Note that during the upward flame propagation driven by re-ignition, the flame edge exhibits the triple flame structure, which is clearly reproduced in the simulations and is illustrated in Fig. 6 (see time instant 9.5 s).

Comparison of the predictions for the two fuel supply rates shows that a smaller flame could be more stable and exist for a longer time than the larger one.

Part 2. Combustion Fundamentals of Fires

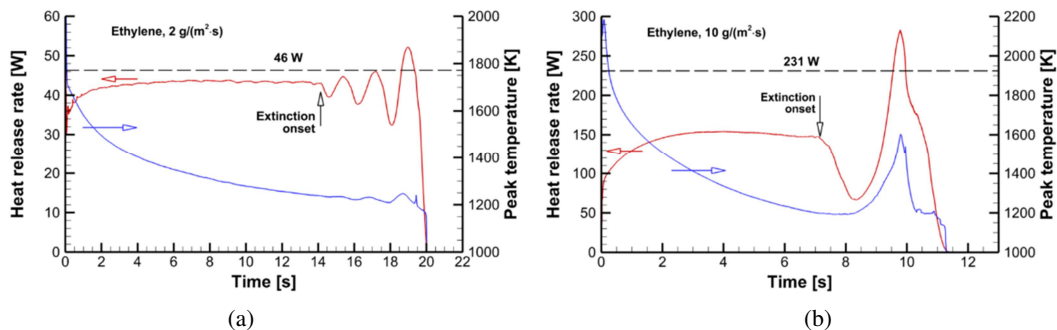


Fig. 9. Predicted transient variations of total heat release rate and peak temperature (100% C_2H_4 , 21% O_2 , 1 bar) at different fuel supply rates: (a) $2\text{ g/(m}^2\cdot\text{s)}$; (b) $10\text{ g/(m}^2\cdot\text{s)}$. Dashed lines show the theoretical heat release rate in complete fuel oxidation.

For the methane flames, a qualitatively similar flame evolution is predicted, although the flame life time was found to be much shorter (two-three times) than that for the ethylene flames. No pronounced oscillating regime was observed after the onset of local flame extinction. Also, the life time of the methane flame is less sensitive to the fuel supply rate. Overall, the ethylene flames are predicted to be more stable and to exist for a longer time than the methane flames (see Fig. 10).

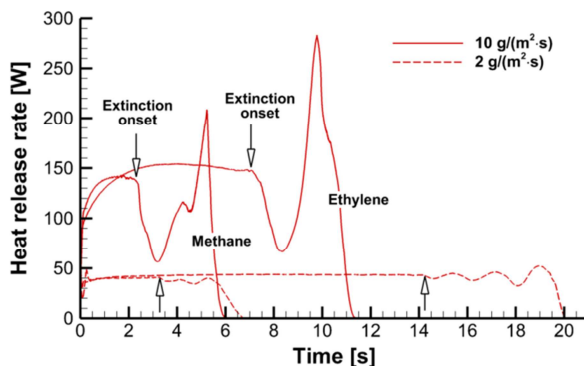


Fig. 10. Predicted transient variations of total heat release rate in methane and ethylene BRE flames at the fuel supply rates 2 and $10\text{ g/(m}^2\cdot\text{s)}$, 21% O_2 , 1 bar. The arrows show the extinction onset.

THE EFFECT OF RADIATIVE LOSSES

To demonstrate the effect of radiative losses, Fig. 11 compares flame shapes predicted with and without radiative emission. With the radiative transfer taken into account, the simulations show that local flame extinction occurs at the flame top in 3 to 4 s after ignition (which is consistent with the drop tower tests). As shown in Fig. 12, fuel is not completely burned (total heat release is well below the theoretical value 49 W), and the peak temperature in the reaction zone gradually decreases until the abrupt drop when the flame is fully extinguished in about 7 s. Dissimilar to that, if radiation is off, then a hot and steady hemispherical flame develops. As shown in Fig. 12, fuel is completely oxidized in such a steady flame, the total heat release is very close to the theoretical value, and the peak temperature approaches the level characteristic of normal gravity diffusion flames. This comparison clearly shows that the flame extinction occurs due to the radiative energy losses from the flame.

In the simulations, the radiative fraction was evaluated as the ratio of the total (volume integral) radiative emission less the radiative absorption to the heat release rate. It can be seen in Fig. 13, that

the radiative fraction steadily grows to the values of about 35 (methane) and 50 (ethylene) percent of the theoretical HRR (corresponding to complete fuel oxidation). As soon as these levels are reached, local extinction occurs. Note that for the actual HRR, corresponding values of the radiative fraction are about 60 and 70%. Further increase of the radiative losses cannot be balanced by the heat release in the reaction zone, and the flame self-extinguishes.

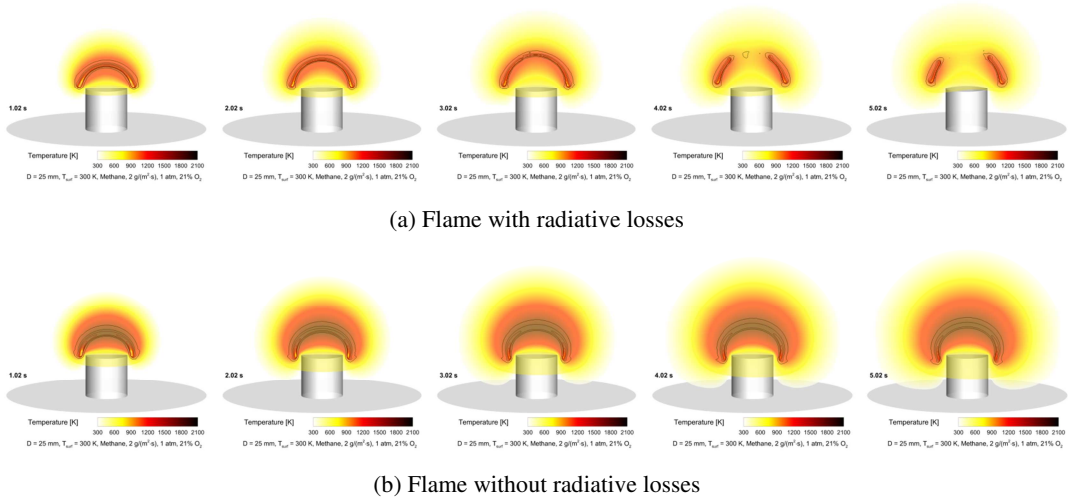


Fig. 11. Predicted temperature distributions and heat release rate iso-curves in the central plane at the time instants 1, 2, 3, 4, and 5 s (100% CH₄, 2 g/(m²·s), 21% O₂, 1 bar).

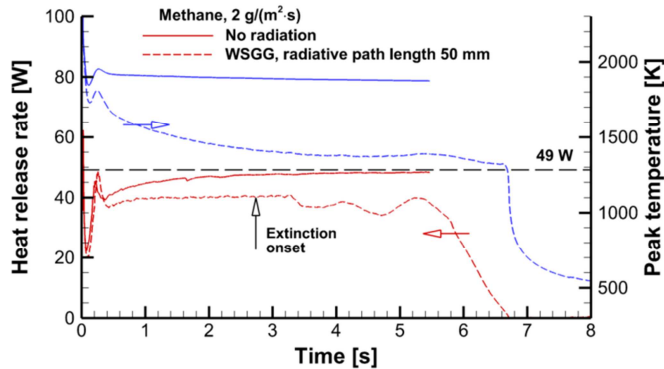


Fig. 12. Predicted transient variations of total heat release rate and peak temperature (100% CH₄, 2 g/(m²·s), 21% O₂, 1 bar) with and without radiative emission. Dashed line shows the theoretical heat release rate in complete fuel oxidation.

To assess the relative contributions by soot and gaseous products, it has to be noticed (see Fig. 6) that soot is only produced during the initial transient period when the flame temperature is sufficiently high (the ethylene flames generate much more soot than the methane flames, as expected). Soot is almost completely oxidized in about 3 s after ignition for both fuels in the considered scenarios. After that, the peak temperatures are rather low and, therefore, soot content is also low. Thus, gas radiation dominates in the zero-gravity BRE flames, and the correct evaluation of the spectral properties of the gaseous combustion products is crucial in predicting radiative emission.

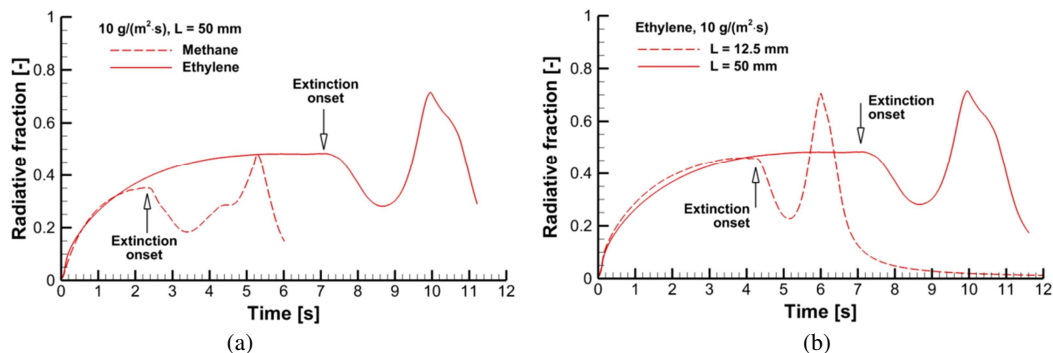


Fig. 13. Predicted transient variations of the radiative fraction (based on the theoretical heat release rate): (a) the effect of fuel; (b) the effect of mean radiation pathlength.

The WSSGG model used in ANSYS Fluent requires the mean radiation pathlength to be assigned in the input data. The simulations have shown that the predicted duration of existence of the steadily growing spherical flame strongly depends on the pre-assigned value of the mean radiation pathlength. Predicted lifetime of the flame ball increases by about 50% as the pathlength is increased from 12.5 mm to 50 mm (see Fig. 13). It is, therefore, instructive to allow for the transient variation of the mean radiation pathlength, which should be coupled with the flame size. Such an algorithm including the steps of (i) identification of the grid cells occupied by the media with the considerable (above the prescribed threshold) radiative emission and calculation of the radiating volume; (ii) evaluation of the area of the surface surrounding the radiating volume; and (iii) determination of the mean radiation path length is currently being developed.

CONCLUSIONS

The main conclusion of this work is that no steady flame has been predicted neither for ethylene nor methane burning above the 25 mm diameter flat circular burner in microgravity. Instead, the simulations have shown that flame development above the BRE burner proceeds in two consecutive modes. First, a hemispherical diffusion flame forms and expands towards a nearly spherical shape. During this time period, flame radius grows almost linearly in time with a minor slowing trend, the heat release rate steadily grows at a slowing growth rate, and the peak temperature steadily decreases from 2100–2200 K down to about 1200 K. In a growing flame, fuel supplied by the burner is only partially burned, and, as a result, the integral HRR is much less than the theoretical value in complete combustion (50 – 70%). The radiative fraction (based on the theoretical HRR) steadily grows to 0.35 (methane) and 0.5 (ethylene) when the local extinction occurs close to the tip of the flame ball.

The second mode is the evolution of the partially extinguished flame. Although complete flame self-extinguishment has been predicted in all the scenarios considered in this work, the extinction scenario depends on the fuel supply rate. In case of small fuel supply rates (2 g/(m²·s)), the extinction is predicted at the top, and the extinguished region propagates downward until the flame dies after several oscillations. For a higher fuel supply rate (10 g/(m²·s)), the extinction dynamics is the same as above except that the re-ignition occurs, and the triple (or hook-like) flame propagates upwards causing bright flash at the top of the flame just before complete self-extinguishment. Both symmetric and asymmetric configurations are possible.

The driving force of flame extinction is the excessive radiative heat loss rate that is not compensated by the heat release rate in the reaction zone. The ethylene flames exist for a longer time period (10 –

12 s) than the methane flames (5 – 6 s), in spite of comparable radiative emission. The latter observation implies that the effect of chemical kinetics is of importance. Smaller flame could be more stable and it could exist for a longer time.

During most part of the time period when the flame exists, the peak temperature in the reaction zone is rather low. This results in a low soot content and, consequently, in a domination of the gas radiation compared to that of soot. When the classical WSGG model is applied to evaluate the effective absorption coefficient of the gaseous combustion products, selection of the mean radiation pathlength strongly affects the prediction of radiative emission from flame and its lifetime prior to extinction.

Based on these blind simulations of the forthcoming orbital experiments, it is anticipated that the microgravity BRE flames should exist for a short time period (or order of 10 s). Pulsations and the bright flash are expected just before complete flame self-extinguishment.

ACKNOWLEDGMENTS

Support by TsNIIMash (Roscosmos) and by RSF research grant 16-49-02017 is gratefully acknowledged. Simulations were performed at the supercomputer center “Polytechnic” (SPbPU).

REFERENCES

- [1] H.D. Ross, Microgravity combustion, Academic Press, San Diego, 2001.
- [2] Y. Zhang, M. Kim, H. Guo, P. B. Sunderland, J. G. Quintiere, J. de Ris, D. P. Stocker, Emulation of condensed fuel flames with gases in microgravity, *Combust. Flame* 162 (2015) 3449–3455.
- [3] Y. Zhang, M. Kim, P. B. Sunderland, J. G. Quintiere, J. de Ris, A burner to emulate condensed phase fuels, *Exp. Therm. Fluid Sci.* 73 (2016) 87–93.
- [4] A. Markan, P. B. Sunderland, J. G. Quintiere, John L. de Ris, D. P. Stocker, H. R. Baum, A Burning Rate Emulator (BRE) for study of condensed fuel burning in microgravity, *Combust. Flame* 192 (2018) 272–282.
- [5] F. V. Lundström, P. B. Sunderland, J. G. Quintiere, P. van Hees, J. L. de Ris, Study of ignition and extinction of small-scale fires in experiments with an emulating gas burner, *Fire Saf. J.* 87 (2017) 18–24.
- [6] Advanced Combustion Microgravity Experiment (ACME), https://www.nasa.gov/mission_pages/station/research/experiments/1908.html
- [7] Space flight experiment Flamenco. TsNIIMash, Roscosmos, 2017, http://knts.tsniimash.ru/ru/site/Experiment_q.aspx?idE=361 (In Russian).
- [8] Snegirev A., Kuznetsov E., Markus E., Markan A., Quintiere J., Sunderland P., De Ris J., Baum H. Simulations of Laminar Diffusion Flames at Normal and Microgravity. BRE-Flamenco project. Work in progress session, 3rd European Symposium on Fire Safety Sciences (ESFSS2018), Nancy, France, 12-14 September 2018, Poster 217947.
- [9] A.Yu. Snegirev, Perfectly stirred reactor model to evaluate extinction of diffusion flame, *Combust. Flame* 162 (2015) 3622–3631.
- [10] A. Kazakov and M. Frenklach, Reduced Reaction Sets based on GRI-Mech 1.2 <http://combustion.berkeley.edu/drm/>
- [11] Z. Luo, C.S. Yoo, E.S. Richardson, J.H. Chen, C.K. Law, T.F. Lu, Chemical explosive mode analysis for a turbulent lifted ethylene jet flame in highly-heated coflow, *Combust. Flame* 159 (2012) 265–274.
- [12] Diffusion Flame Measurements, NIST archive <https://www.nist.gov/el/fire-research-division-73300/diffusion-flame-measurements>, 1999.
- [13] GRI-Mech 3.0 <http://combustion.berkeley.edu/drm/>
- [14] BRE test video archive https://www.youtube.com/user/akshit05/videos?disable_polymer